Solid State Electronics 155 (2019) 93–98

Contents lists available at ScienceDirect

Solid State Electronics

journal homepage: www.elsevier.com/locate/sse

Nanoelectronics with proximitized materials

Igor Žutić[a,*], Alex Matos-Abiague[b], Benedikt Scharf[c], Tong Zhou[a], Hanan Dery[d], Kirill Belashchenko[e]

[a] Department of Physics, University at Buffalo, State University of New York, Buffalo, NY 14260, USA
[b] Department of Physics and Astronomy, Wayne State University, Detroit, MI 48201, USA
[c] Institute for Theoretical Physics and Astrophysics, University of Wurzburg, Am Hubland, 97074 Würzburg, Germany
[d] Department of Electrical and Computer Engineering, and Department of Physics and Astronomy, University of Rochester, NY 14627, USA
[e] Department of Physics and Astronomy, and Nebraska Center for Materials and Nanoscience, University of Nebraska-Lincoln, NE 68588-0299, USA

ARTICLE INFO

The review of this paper was arranged by Profs. S. Luryi, J. M. Xu, and A. Zaslavsky

Keywords:
Proximity effects
Spintronics
Superconductors
Majorana bound states
Spin valves

ABSTRACT

While materials design for many device applications usually relies on adding impurities, recent advances in scaling-down heterostructures with improved interfacial properties offer a different way to transform a large class of materials. A given material can be drastically changed by inheriting properties leaking from its neighboring regions, such as magnetism, superconductivity, or spin-orbit coupling. While these proximity effects often have a short range and are considered negligible, the situation is qualitatively different in atomically thin and two-dimensional materials where the extent of proximity effects can exceed their thickness. Consequently, proximitized materials have a potential to display novel properties and device opportunities, absent in any of the constituent region of the considered heterostructures. Such proximitized materials could provide platforms for a wide range of emerging applications: from seamless integration of memory and logic, to fault-tolerant topologically protected quantum computing.

1. Introduction

The appeal of common semiconductors, such as Si or GaAs, often comes from the ability to strongly alter their properties through doping, when impurities are intentionally introduced. Just like many other materials, in their pristine form semiconductors are usually of a limited use. Instead, their doping is critical for a large class of devices: solar cells, light emitting diodes, transistors, and lasers [1,2]. More than just in semiconductors, chemical doping is widely recognized as an effective method to drastically change many other materials: from insulators and metals, to topological insulators and high-temperature superconductors.

Continued scaling-down of nanoelectronics and recent advances in fabricating high-quality epitaxial heterostructures offer a completely different path to transform a large class of materials through proximity effects. The concept of such “proximitized materials” [3], is realized by recognizing that a given material can be transformed by inheriting properties from its neighboring regions, as depicted in Fig. 1. For example, layer B can acquire proximity-induced superconductivity and magnetism, “leaking” from the neighboring regions. The outcome in such proximitized materials can be unexpected as they can demonstrate novel properties and device opportunities, absent in any of the constituent region of the considered heterostructures.

Historically, the intuition about proximity effects comes from the superconducting case already discovered by Holm and Meissner in 1932 [4]. While limited to low temperatures, in contrast to other proximity effects that typically persist only within a nm scale, the superconducting proximity effect can extend many μm in the interior of a non-superconducting region. This “leaking” superconductivity, depicted in Fig. 2(a), resembles also a magnetic proximity effect where the magnetism penetrates into an initially nonmagnetic region. High interfacial quality and transparency are common prerequisites for various proximity effects, a large barrier between the regions could diminish such leaking. A microscopic picture of superconducting proximity effects comes from the peculiar process of Andreev reflection, inherent to superconducting interfaces [5]. For a normal metal/superconductor (N/S) junction, there is a specular (ordinary) reflection, similar to a ball bouncing of a wall. In this case an electron approaching the N/S interface is reflected with the same charge and the same spin. In contrast, during Andreev reflection illustrated in Fig. 2(b), an electron approaching the interface is reflected backwards and converted into a hole (the absence of an electron is depicted as an empty circle) with opposite charge and spin. From the charge conservation we infer that two electron charges are transferred across the interface into the S

* Corresponding author.
E-mail address: zigor@buffalo.edu (I. Žutić).

https://doi.org/10.1016/j.sse.2019.03.015

Available online 05 March 2019
0038-1101/ © 2019 Elsevier Ltd. All rights reserved.

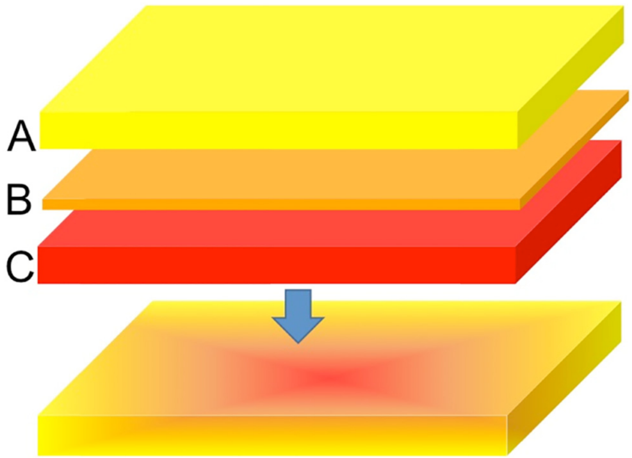

Fig. 1. Proximity modified layer B in the presence of layers A, C. The resulting properties of the layer B can be very different from those in layers A and C.

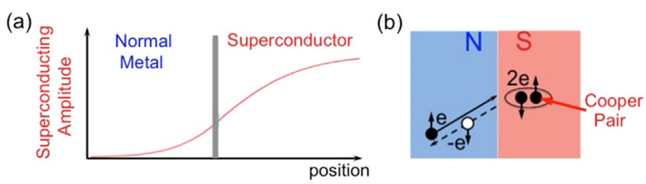

Fig. 2. (a) Penetration of superconductivity across an interface into a normal (nonsuperconducting) region. (b) Andreev reflection at the N/S interface. The incident electron is reflected as a hole which retraces the initial trajectory and the two electrons are transferred to the super-conducting region. From the energy conservation, an incident electron, slightly above the Fermi level is accompanied by another electron of opposite spin slightly below the Fermi level. The transfer of the second electron below the Fermi level into a superconductor is equivalent to a reflected hole moving away from the N/S interface.

region. These two electrons with opposite spins form a Cooper pair. Since the reflected particle carries the information about both the phase of the incident particle and the macroscopic phase of the superconductor to which a Cooper pair is being transferred, Andreev reflection is thus responsible for the proximity effect in which the phase correlations are introduced to a nonsuperconducting material [6].

An important manifestation of the superconducting proximity is the Josephson effect [7]. It relies on proximity-induced superconductivity across a normal region sandwiched between two superconductors. Once the voltage is applied across this device, a dissipationless supercurrent flows. Such a Josephson junction is the key element of a superconducting quantum interference device (SQUID) [8] that provides extremely sensitive detection of magnetic fields (as small 10^{-17} T) finding its use from the studies of biological systems and magnetic resonance imaging, to the detection of gravitational waves [9].

2. Adding spin to electronics

While spin and its associated magnetic moment is an intrinsic property of electrons, conventional electronics is oblivious to it. Without an applied magnetic field or magnetic materials, there is a balance of carriers with spin up and down directions, therefore their spin can be ignored. On the other hand, in spin electronics or spintronics [6,10–14], magnetic materials and spin-dependent properties provide important device opportunities. Ferromagnetic metals such as iron or cobalt have a finite magnetization, their electrons' spins are oriented either with or against the magnetization axis, depending on the material. This magnetization direction persists without an outlet power and is therefore nonvolatile. Commercial spintronic applications are based on ferromagnetic metals which utilize magnetoresistive effects for magnetically storing and sensing information, such as computer hard drives, magnetic sensors, and magnetic random access memory (MRAM) [6,10,13,14]. However, this may only be the tip of the iceberg. A versatile control of spin and magnetism in a wide class of materials and their nanostructures could also have a much broader impact leading to novel devices for communication or logic and even fault-tolerant quantum computing [6,15–20].

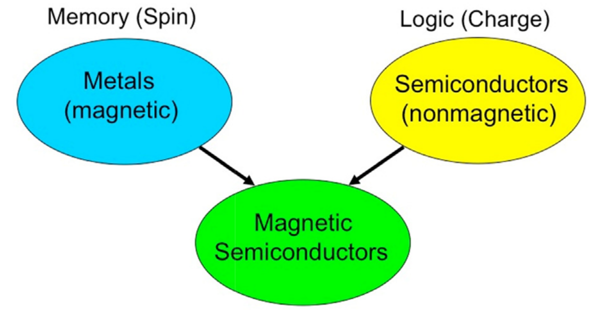

Fig. 3. A motivation for investigating magnetic semiconductors that could potentially integrate, in a single materials system, memory and logic.

Given the respective success of conventional semiconductors to implement charge-based logic and ferromagnetic metals for spin-based nonvolatile memory, there is hope that by combining the control of charge and spin in a single material, as shown in Fig. 3, would provide more than just the sum of its separate parts (charge and spin) and enable new or improved functionalities. This was the key motivation behind several decades of research in dilute magnetic semiconductors (DMS), where by magnetic doping, typically using Mn, of nonmagnetic semiconductor host it is possible to realize carrier-mediated magnetism [6,21,22]. DMS offer a control of the exchange interaction by tuning the ferromagnetic Curie temperature, T_C, through changes in the carrier density, by an applied electric field and photoexcitation [6,22–26].

However, this effort to add spin into electronics comes with significant obstacles. In (Ga,Mn)As, the most common III-V DMS, Mn^{2+} leads to both spin and carrier doping enabling a T_C of up to ~200 K [27], but limited by a low Mn^{2+} solubility which complicates its growth and can create nanoscale clustering of Mn ions. Instead of the desired single phase (Ga,Mn)As, the outcome of the growth could yield nonmagnetic semiconductor GaAs accompanied by nanonoclusters of ferromagnetic metal MnAs having a magnetic signal mistaken with (Ga,Mn)As [6]. This dual role of Mn as both spin and carrier doping creates a strong perturbation and disorder in the nonmagnetic host, reducing its mobility by 2–3 orders of magnitude [6] and significantly degrading excellent optical properties of GaAs such that (Ga,Mn)As has a negligible luminescence. While the efforts to improve DMS continue by considering a novel II-II-V DMS class, such as $(Ba,K)(Zn,Mn)_2As_2$ [28–30], which provide an independent spin and charge doping, as well as exploring (III,Fe)V systems which can push T_C up to ~330 K [31], the challenges of reduced mobility and degraded optical properties remain.

An alternative path to add spin and magnetism in nonmagnetic materials is through magnetic proximity effects [3,32], they could overcome degrading the properties of a nonmagnetic host (such as strong disorder, low mobility, and weak luminescence) accompanied by doping. Furthermore, magnetic proximity can also strongly increase T_C in DMS, shown to exceed 400 K when (Ga,Mn)As was placed next to Co_2FeAl [33]. To better understand challenges and opportunities for using proximity effects, it is useful to note that while they usually imply equilibrium properties (zero bias), they can also alter nonequilibrium properties of materials. For magnetic proximity effects, magnetism will already leak into a nonmagnetic material at zero bias, resulting in different spin up and spin down properties (with respect to the direction of a magnetization or an applied magnetic field), while at finite bias,

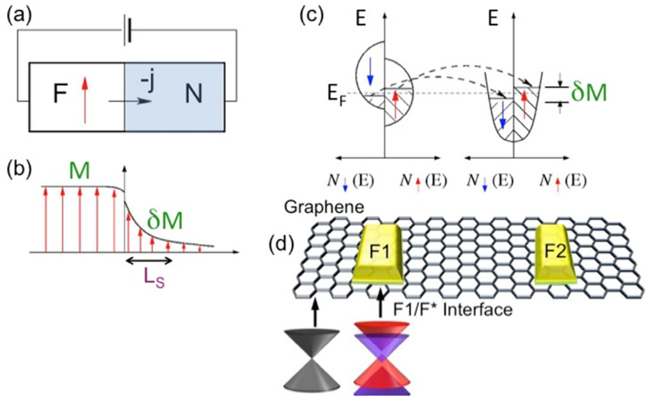

Fig. 4. (a) Spin injection from a ferromagnet (F) into a nonmagnetic region (N). Electrons flow from F to N (opposite to the current j). (b) Spatial dependence of the magnetization M, nonequilibrium magnetization δM (spin accumulation) decays in N over the spin diffusion length, L_S. (c) Contribution of different spin-resolved DOS to both charge and spin transport across the F/N interface leads to δM. (d) Magnetic proximity effects in F1/graphene junction. The electronic structure of proximity-modified graphene, F* becomes spin-dependent. A ferromagnet, F2, can be used for detecting magnetic proximity effects through transport. Adapted from Ref. [3]. motivation for investigating magnetic semiconductors that could potentially integrate, in a single materials system, memory and logic.

even nonequilibrium properties will be proximity-modified, including the charge current.

It is useful to contrast magnetic proximity effect from electrical spin injection [6], a transport method for generating nonequilibrium spin, shown in Fig. 4(a)–(c). A ferromagnet (F) has a net magnetization M and differenet spin-up and spin-down density of states (DOS). When a charge current flows across the F/nonmagnetic region (N) junction, spin-polarized carriers in a ferromagnet contribute to the net current of magnetization entering N, resulting in the nonequilibrium magnetization δM, also known as the spin accumulation [6]. A characteristic length scale for δM is the spin diffusion length, $L_S > 100$ nm in many materials, while in graphene it can even exceed 30 μm at 300 K [34]. Given that a typical lengthscale for magnetic proximity effects is ~nm, orders of magnitude shorter than L_S, they seems completely negligible in transport properties of F/N junctions.

However, the situation is qualitatively different for an atomically thin N region, illustrated on the example of graphene in Fig. 4(d). The thickness of graphene as well as other monolayer van der Waals materials is smaller than the characteristic magnetic proximity length and thus in such a geometry interface and proximity effects become crucial [3]. A part of the N region next to the F (metallic or insulating) is transformed by the magnetic proximity effects acquiring across its thickness equilibrium spin-dependent properties, which also directly modify the nonequilibrium properties including the flow of current or optical excitation in that region. The process of spin injection is no longer from the F to N region, but from F to the proximity-modified region F* [35]. For graphene, as shown in Fig. 4(d), such F* could lead to the proximity-induced exchange splitting of a Dirac cone. The nonequilibrium (transport) properties, including the flow of charge and spin current, as well as spin accumulation, will depend on the proximity-induced exchange splitting in F* below F1. It is helpful to distinguish two mechanisms for magnetic proximity effects [36]: (i) The wave functions from graphene penetrate into the insulating F as evanescent states since there are no states there at the Fermi level, where they acquire exchange splitting from its native ferromagnetism. (ii) The wave functions from the metallic F penetrate into graphene, directly polarizing its electronic structure at the Fermi level.

A spin accumulation and spin-polarized currents are readily detected by placing another F, i.e. in the F1/N/F2 geometry, as shown in

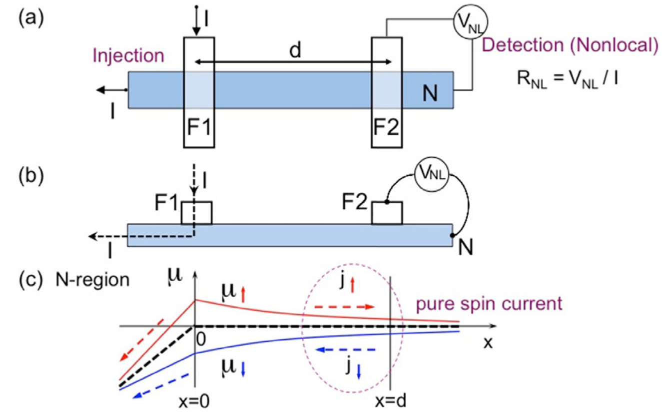

Fig. 5. Spin injection and nonlocal detection in a lateral spin-valve device. (a) Top and (b) side view. The bias current, I, flows from F1 to the left end of N, the spin signal is detected by measuring a nonlocal voltage, V_{NL} between F2 and N. V_{NL} and the nonlocal resistance, $R_{NL} = V_{NL}/I$, depend on the relative orientation of **M** in F1 and F2. (c) A spatial dependence of electrochemical potential μ (broken line) and its spin-resolved components in N. For $x > 0$, there is no net charge current density, $j\uparrow + j\downarrow$, but as a result of spin diffusion and δM, only pure spin current, $j\uparrow - j\downarrow$, flows. Adapted from Ref. [3].

Fig. 5. Using a nonlocal geometry pioneered by the work of Johnson and Slisbee [37,38], spin injection is spatially separated from spin detection to eliminate spurious effects attributed to spin transport [39,40]. Subsequently, this approach has been extended to many different materials, including graphene [41,42]. Driven by the spin accumulation and thus δM, in the equipotential region $x > 0$, there is a flow of pure spin current, $j\uparrow - j\downarrow$, with the spin-resolved current density, $j\uparrow, j\downarrow$, proportional to the slope of $\mu\uparrow,\downarrow$. Both the flow of spin and charge current, as well as spin accumulation depend on the relative orientation of **M** in F1 and F2.

In a lateral device similar to that from Fig. 5, with 3 F contacts were made of Co, separated by a tunnel barrier MgO from graphene sheet as the N region, spin logic was demonstrated at 300 K [43]. An important potential of similar devices is to enable a paradigm change from the von Neumann architecture to one in which memory and processing are seamlessly integrated together. While in the current implementation graphene-based spin logic relies on the applied magnetic field to change the magnetic configuration in F electrodes, this is not a fundamental constraint. It was predicted that with gate voltage DOS spin polarization induced in graphene through magnetic proximity effects can change its magnitude as wells reverse its sign [36]. Therefore, rather than reversing the magnetization configuration with applied magnetic field, it may be possible to employ all-electrical control of magnetic proximity effects. The feasibility of such approach has been supported by the room temperature magnetic proximity effects in graphene, using both ferromagnetic metals and insulators [44,45], as well in a geometry of 1D edge Co contacts showing a reversal of proximity-induced spin polarization [46].

3. Multiple proximity effects: Majorana bound states

Important implications for optoelectronic devices arise from the well-known quantum mechanical properties of electrons and photons. A different symmetry of the wavefunction under exchange of two identical particles leads to the simple phase change: π for electrons and zero for photons, as expected for fermions and bosons, respectively. A qualitatively different situation is possible for Majorana zero modes, also known as the Majorana bound states (MBS), exotic composite particles (quasiparticles) which are neither fermions, nor bosons [20,47]. They have been inspired by the prediction of Majorana fermions, γ, in high-energy physics [48] that are their own antiparticles $\gamma = \gamma^+$ (described by real, rather than complex, wavefunction) and thus are zero energy,

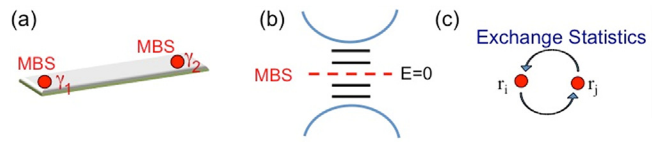

Fig. 6. (a) A spatially-separated pair of Majorana bound states (MBS) at the ends of a wire represents a single electron, protected from local perturbations. (b) MBS have zero energy and are protected by a superconducting gap from the other states. (c) Under exchange the MBS wavefunction behaves entirely different from bosons or fermions and displays a non-Abelian statistics.

chargeless, and spinless [49].

MBS properties in solid-state systems are even more exotic. One MBS can be viewed as a half of an electron, but such a fermion is made two spatially separated and localized MBS ($f = \gamma_1 + i\ \gamma_2$) and thus protected from local perturbations, typical for the operation of electronic devices, that would affect only one of its MBS constituents. This situation is depicted in Fig. 6. A pair of MBS constitutes a two-state system, just like a spin ½ electron. Remarkably, MBS are characterized by a non-Abelian (non-commutative) statistics: under MBS exchange the resulting wavefunction does not simply acquire a phase change as for fermions or bosons, instead it is transformed into another wavefunction similar to a matrix multiplication. This points to an intriguing possibility to use the exchange (braiding) of MBS as an implementation of a topologically-protected quantum gate [50,51], resulting in efforts in topological quantum computing actively pursed by some major information technology companies. In this context the term "topological protection," similar to a knot which is preserved under small continuous movements of the rope, brings about global properties and physical behavior that is robust under external perturbations and disorder.

While it is recognized that superconductors are a natural platform to realize chargeless states, similar to the mixing of electrons and holes through Andreev reflection [recall Fig. 2(b)], a further requirement for a spinless character of MBS is elusive in nature. Unlike typical spin-singlet Cooper pairs, spin-triplet pairing superconductivity would be needed. Instead, the desired spin structure of MBS can be implemented in proximity-induced superconductivity in semiconductors with strong spin-orbit coupling (SOC) and applied magnetic field, which can create an effective spin-orbit coupling (SOC) and applied magnetic field, which can create an effective spin-triplet [52–54]. The most developed MBS platforms rely on common superconductors that induce superconductivity in narrow bandgap semiconductor nanowires [55–57]. However, such detection is indirect, typically relying on a zero-bias conductance peak [55–60], predicted to be quantized [61], rather than probing directly their non-Abelian statistics. The existing 1D geometries also pose additional obstacles to realize braiding and fusing of MBS, the key elements for topological quantum computing.

To address these challenges, we propose that a versatile control of magnetic systems, widely used to store information, for example, in MRAM, can also enable manipulating MBS [62,63]. Our platform, depicted in Fig. 7, relies on the proximity-induced superconductivity in a 2D electron gas (2DEG) that is further modified by the magnetic proximity effects from an array of magnetic tunnel junctions (MTJs) [62]. A change in the magnetization configuration in the MTJ array creates tunable magnetic textures and the resulting fringing fields, thereby removing several typical requirements for MBS: applied magnetic field, strong SOC, and confinement by 1D structures which complicates demonstrating non-Abelian statistics. To see that we consider changes in the 2DEG due to the nearby magnetic array. The corresponding Zeeman term in the Hamiltonian, $\sim \mathbf{B}(\mathbf{r})\cdot\sigma$, where a magnetic textures is represented by a spatially inhomogeneous effective magnetic field, $\mathbf{B}(\mathbf{r})$, and σ is the vector of Pauli matrices, can be diagonalized by performing local spin rotations aligning the spin quantization axis to the local magnetic field direction. In the rotated frame, a simple

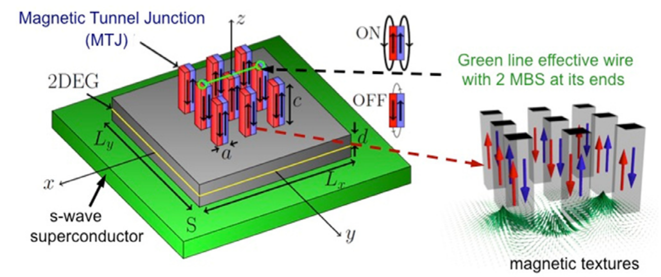

Fig. 7. Schematic of the setup. A two-dimensional electron gas (2DEG) is formed in a semiconductor quantum well grown on the surface of an s-wave superconductor (S). An array of magnetic tunnel junctions (MTJs) produces a magnetic texture, tunable by switching individual MTJs to the parallel (ON) or antiparallel (OFF) configuration. For the depicted array configuration, two MBS form at the ends of the middle row (green curve). Adapted from Ref. [62].

diagonal term $|\mathbf{B}(\mathbf{r})|\sigma_z$ of a collinear Zeeman interaction acts similar to an externally applied magnetic field. This simplification is also accompanied by additional terms in the transformed Hamiltonian involving a non-Abelian vector potential which can be interpreted as the synthetic SOC [62–65]. Furthermore, as can also be inferred from a piecewise constant $\mathbf{B}(\mathbf{r})$, magnetic textures can provide a confinement without the need for physical wires. With tunable magnetic textures it may then be possible to confine and reposition MBS [62].

In a 1D semiconductor nanowire geometry, a well-known topological condition required for MBS formation is $B \sim E_{Zeeman} \geq (\mu^2 + \Delta^2)^{1/2}$ [53,54], where Δ is the proximity-induced superconducting gap, typically a fraction of meV. While large B and thus Zeeman energy, E_{Zeeman}, would then appear desirable, B should also be chosen carefully such that it is not too large to destroy superconductivity. In our case this topological condition should be also generalized [62,63]: $\mu^2 \rightarrow [\mu - \eta(r)]^2$, where $\eta(r)$ represents an effective shift in chemical potential due to local changes of the magnetic texture. In the limit of a homogeneous magnetic field, $\eta \rightarrow 0$ [62]. Consequently, changing the magnetic configuration of an MTJ array (as in Fig. 7) will modify the generalized topological condition. When such a condition attains equality, it can define a reconfigurable effective topological wire which hosts MBS localized at its ends.

Fig. 8 illustrates the formation of such topological wires (white contours) in a 2DEG transformed by superconducting (from a conventional superconductor) and magnetic proximity effects (from 3 × 3 MTJ array), as shown in Fig. 7. As the wires are reconfigured, MBS can be repositioned and braided [62,63]. The potential advantages of the proposed MTJ-based platform can be summarized as follows: (i) no restrictive geometries such as physical wires (epitaxially defined) are required, (ii) the magnetic textures can be locally controlled by electrical switching of individual MTJs (i.e., no external magnetic fields are needed) and (iii) no contacts are required for manipulating MBS, minimizing the risk of quasiparticle poisoning [20], a source of MBS decoherence. Recent advances in fabricating 2D epitaxial superconductor/semiconductor (Al/InAs) heterostructures and designing tunable magnetic textures support the feasibility of this platform for MBS [66,67]. Various other realizations of the interplay between proximity-induced superconductivity and magnetism continue to be pursued in the quest to realize and control MBS [68–73]. Efforts to fabricate transparent superconducting junctions with topological insulators [74] with large proximity-induced gaps as well as other implementations of Josephson junctions [75–78] could provide additional opportunities to use magnetic textures to realize non-Abelian MBS properties and theoretically study how to optimize such systems using the combination of intrinsic and synthetic SOC [79,80].

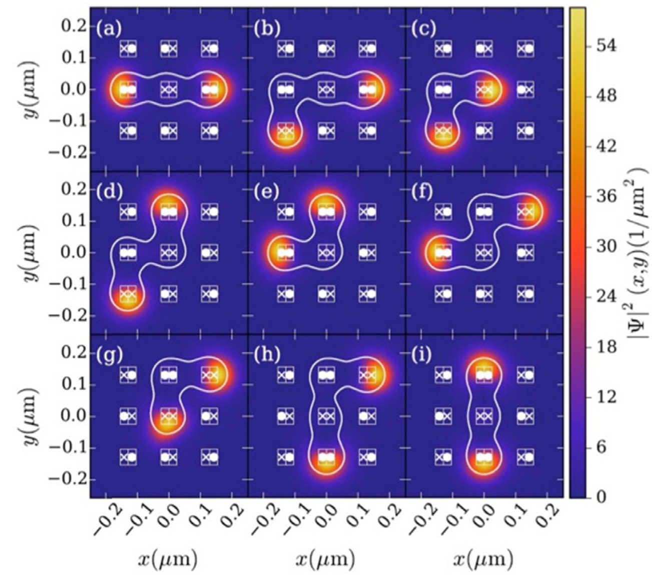

Fig. 8. Probability densities of the MBS for the initial state (a) and of the first eight stable configurations of the MTJ array [(b)–(i)], S_0; …; S_8, superimposed with magnetization [white rectangles with dots (crosses) for the direction parallel (anti-parallel) to the z axis]. The effective wires are marked with white contours [20]. Adapted from Ref. [62].

4. Conclusions

Using proximity effects to transform materials allows us to revisit various paths to realize emerging nanoelectronic devices and even implement elusive topologically-protected properties. This push is further stimulated by a growing number of 2D van der Waals materials with atomically sharp interfaces and gate-tunable properties which form heterostructures that are not limited by the usual lattice matching constraints expected for conventional semiconductors [81,82]. Many opportunities are still largely unexplored as has been recently seen that with a simple change in the relative stacking (a twist angle) a bilayer graphene becomes superconducting or displays strong correlations [83,84]. Beyond a widely-used graphene, insulator h-BN, and transition metal dichalcogenides as direct bandgap semiconductors, a variety of proximity effects is expanded by the monolayer superconductors and ferromagnets [81,82,85–88]. Even short-range magnetic proximity effects are sufficient for atomically thin structures to undergo crucial changes at room temperatures. Employing tunable magnetic proximity effects, which strongly modify transport and optical properties in van der Waals materials [89–91], one can envision high-performance spin interconnects [3] and ultrafast spin lasers [92], important for addressing power consumption in contemporary computers that is increasingly dominated by information transfer, rather than logic [93].

Acknowledgments

We thank G. Fatin, G. Xu, J. Shabani and A. D. Kent for valuable discussions. This work was supported by the U.S. ONR, 000141712793 (I.Ž., A.M-A.), DARPA, D18AP900007 (I.Ž., A.M-A.), U.S. DOE, Basic Energy Sciences, DE-SC0004890 (I.Ž., T.Z.), NSF ECCS-1810266 (I.Ž.), DFG SFB 1170 “ToCoTronics” (B.S.) and ENB Graduate School on Topological Insulators (B.S.), U.S. DOE, Basic Energy Sciences, Award DE-SC0014349 (H.D.), NSF DMR-1503601 (H.D.), DTRA HDTRA1-13-1-0013 (H.D.), NSF DMR-1609776 (K.B.) and the Nebraska MRSEC, DMR-1420645 (K.B.).

Appendix A. Supplementary data

Supplementary data to this article can be found online at https://doi.org/10.1016/j.sse.2019.03.015.

References

[1] Alferov ZH. Nobel Lecture: the double heterostructure concept and its applications in physics, electronics, and technology. Rev Mod Phys 2001;73:767.
[2] Yu PY, Cardona M. Fundamentals of semiconductors: physics and materials properties. fourth ed. Berlin: Springer; 2010.
[3] Žutić I, Matos-Abiague A, Scharf B, Dery H, Belashchenko K. Proximitized materials. Mater Today 2019;22:85. https://doi.org/10.1016/j.mattod.2018.05.003. (open access).
[4] Holm R, Meissner W. Messungen mit Hilfe von flüssigem Helium. XIII. Z Phys 1932;74:75.
[5] Andreev AF. The thermal conductivity of the intermediate state in superconductors. Zh Eksp Teor Fiz 1964;46:1823. [Sov. Phys. JETP 19, 1228 (1964)].
[6] Žutić I, Fabian J, Das Sarma S. Spintronics: fundamentals and applications. Rev Mod Phys 2004;76:323.
[7] Josephson BD. Possible new effects in superconductive tunneling. Phys Rev Lett 1962;1:251.
[8] Tinkham M. Introduction to superconductivity. New York: McGraw-Hill; 2011.
[9] Romani GL, Williamson SJ, Kaufman L. Biomagnetic instrumentation. Rev. Sci. Instrum. 1982;53:1815. M. Goryachev, M.E. Tobar, Gravitational wave detection with high frequency phonon trapping acoustic cavities, Phys. Rev. D 90, 102005 (2014).
[10] Sverdlov V, Sleberherr S. Silicon spintronics: progress and challenges. Phys Rep 2015;85:1.
[11] Fabian J, Mathos-Abiague A, Ertler C, Stano P, Žutić I. Semiconductor spintronics. Acta Phys Slov 2007;57:565.
[12] Das Sarma S, Fabian J, Hu XD, Žutić I. Spin electronics and spin computation. Solid State Commun 2001;119:207.
[13] Tsymbal EY, Žutić I, editors. Handbook of Spin Transport and Magnetism. Boca Raton, FL: Taylor & Francis/CRC Press; 2012.
[14] Maekawa S, editor. Concepts in Spin Electronics. Oxford: Oxford University Press; 2006.
[15] Dery H, Song Y, Li P, Žutić I. Silicon spin communication. Appl Phys Lett 2011;99:082502.
[16] Dery H, Dalal P, Cywinski L, Sham LJ. Spin-based logic semiconductors for reconfigurable large-scale circuits. Nature 2007;447:573.
[17] Rangaraju N, Peters JA, Wessels BW. Magnetoamplification in a bipolar magnetic junction transistor. Phys Rev Lett 2010;105:117202.
[18] Fabian J, Žutić I, Das Sarma S. Magnetic bipolar transistor. Appl Phys Lett 2004;84:85.
[19] Dery H, Wu H, Ciftcioglu B, Huang M, Song Y, Kawakami R, et al. Spintronic nanoelectronics based on magneto-logic gates. IEEE Trans Electron Dev 2012;59:259.
[20] Aasen D, Hell M, Mishmash RV, Higginbotham A, Danon J, Leijnse M, et al. Milestones toward Majorana-based quantum computing. Phys Rev X 2016;6:031016.
[21] Furdyna JK. Diluted magnetic semiconductors. J Appl Phys 1988;64:R29.
[22] Dietl T, Ohno H. Dilute ferromagnetic semiconductors: physics and spintronic structures. Rev Mod Phys 2014;86:187.
[23] Koshihara S, Oiwa A, Hirasawa M, Katsumoto S, Iye Y, Urano S, et al. Ferromagnetic order induced by photogenerated carriers in magnetic III-V semiconductor heterostructures of (In, Mn)As/GaSb. Phys Rev Lett 1997;78:4617.
[24] Ohno H, Chiba D, Matsukura F, Abe TOE, Dietl T, Ohno Y, et al. Electric-field control of ferromagnetism. Nature 2000;408:944.
[25] Cabral ED, Boselli MA, Oszwaldowski R, Žutić I, da Cunha Lima IC. Electrical control of magnetic quantum wells – Monte Carlo simulations. Phys Rev B 2011;84:085316.
[26] Anh LD, Hai PN, Kasahara Y, Iwasa Y, Tanaka M. Modulation of ferromagnetism in (In, Fe)As quantum wells via electrically controlled deformation of the electron wave function. Phys Rev B 2015;92:161201(R).
[27] Chen L, Yang X, Yang F, Zhao J, Misuraca J, Xiong P. Enhancing the Curie temperature of ferromagnetic semiconductor (Ga, Mn)As to 200 K via nanostructure engineering. Nano Lett 2011;13:2584.
[28] Zhao K, et al. New diluted ferromagnetic semiconductor with Curie temperature up to 180 K and isostructural to the ‘122’ iron-based superconductors. Nat Commun 2013;4:1442.
[29] Zhao K, et al. Ferromagnetism at 230 K in $(Ba_{0.7}aK_{0.3})(Zn_{0.85}Mn_{0.15})_2As_2$ diluted magnetic semiconductor. Chin Sci Bull 2014;59:2524.
[30] Zhao GQ, et al. Single crystal growth and spin polarization measurements of diluted magnetic semiconductor $(Ba,K)(Zn,Mn)_2As_2$. Sci Rep 2017;7:14473.
[31] Tu NT, Hai PN, Anh LD, Tanaka Masaaki. High-temperature ferromagnetism in new n-type Fe-doped ferromagnetic semiconductor (In,Fe)Sb. Appl Phys Exp 2018;11,:063005.
[32] Hauser JJ. Magnetic proximity effect. Phys Rev 1969;187:580.
[33] Nie SH, et al. Ferromagnetic interfacial interaction and the proximity effect in a Co_2FeAl/(Ga, Mn)As bilayer. Phys Rev Lett 2013;111:027203.
[34] Drogler M, et al. Spin lifetimes exceeding 12 ns in graphene nonlocal spin valve devices. Nano Lett 2016;16:3533.
[35] Lazić P, Sipahi GM, Kawakami RK, Žutić I. Graphene spintronics: Spin injection and proximity effects from first principles. Phys Rev B 2014;90:085429.

[36] Lazić P, Belashchenko KD, Žutić I. Effective gating and tunable magnetic proximity effects in two-dimensional heterostructures. Phys Rev B 2016;93:241401(R).
[37] Johnson M, Silsbee RH. Interfacial charge-spin coupling: Injection and detection of spin magnetization in metals. Phys Rev Lett 1985;55:1790.
[38] Johnson M, Silsbee RH. Thermodynamic analysis of interfacial transport and of the thermomagnetoelectric system. Phys Rev B 1987;35:4959.
[39] Song Y, Dery H. Magnetic-field-modulated resonant tunneling in ferromagnetic-insulator-nonmagnetic junctions. Phys Rev Lett 2014;113:047205.
[40] Maekawa S, Valenzuela S, Saitoh E, Kimura T, editors. Spin Current. New York: Oxford University Press; 2012.
[41] Tombros N, Józsa C, Popinciuc M, Jonkman HT, van Wees BJ. Electronic spin transport and spin precession in single graphene layers at room temperature. Nature 2007;448:571.
[42] Józsa C, van Wees BJ. Graphene Spintronics. In: Tsymbal EY, Žutić I, editors. Handbook of Spin Transport and Magnetism. Boca Raton, FL: Taylor & Francis/CRC Press; 2012. p. 579–98.
[43] Wen H, Dery H, Amamou W, Zhu T, Lin Z, Shi J, et al. Experimental demonstration of XOR operation in graphene magnetologic gates at room temperature. Phys Rev Appl 2016;5:044003.
[44] Leutenantsmeyer JC, Kaverzin AA, Wojtaszek M, van Wees BJ. Proximity induced room temperature ferromagnetism in graphene probed with spin currents. 2D Mater 2017;4:014001.
[45] Asshoff PU, et al. Magnetoresistance of vertical Co-graphene-NiFe junctions controlled by charge transfer and proximity-induced spin splitting in graphene. 2D Mater 2017;4:031004.
[46] Xu J, Singh S, Katoch J, Wu G, Zhu T, Žutić I, et al. Spin inversion in graphene spin valves by gate-tunable magnetic proximity effect at one-dimensional contacts. Nat Commun 2018;9:2869.
[47] Kitaev A. Fault-tolerant quantum computation by anyons. Ann Phys 2003;303:2.
[48] Elliott SR, Franz M. Colloquium: Majorana fermions in nuclear, particle, and solid-state physics. Rev Mod Phys 2015;87:137.
[49] Alicea J. New directions in the pursuit of Majorana fermions in solid state systems. Rep Prog Phys 2012;75:076501.
[50] Das Sarma S, Freedman M, Nayak C. Majorana zero modes and topological quantum computation. Quantum Inf. 2015;1:15001.
[51] Nayak C, Simon SH, Stern A, Freedman M, Das Sarma S. Non-Abelian anyons and topological quantum computation. Rev Mod Phys 2008;80:1083.
[52] Fu L, Kane CL. Superconducting proximity effect and Majorana fermions at the surface of a topological insulator. Phys Rev Lett 2008;100:096407.
[53] Lutchyn RM, Sau JD, Das Sarma S. Majorana Fermions and a topological phase transition in semiconductor-superconductor heterostructures. Phys Rev Lett 2010;105:077001.
[54] Oreg Y, Refael G, von Oppen F. Helical liquids and Majorana bound states in quantum wires. Phys Rev Lett 2010;105:177002.
[55] Mourik V, Zuo K, Frolov SM, Plissard SR, Bakkers EPAM, Kouwenhoven LP. Signatures of Majorana fermions in hybrid superconductor-semiconductor nanowire devices. Science 2012;336:1003.
[56] Albrecht SM, Higginbotham AP, Madsen M, Kuemmeth F, Jespersen TS, Nygard J, et al. Exponential protection of zero modes in Majorana islands. Nature 2016;531:206.
[57] Zhang H, et al. Quantized Majorana conductance. Nature 2018;556:74.
[58] Pawlak R, Kisiel M, Klinovaja J, Meier T, Kawai S, Glatzel T, et al. Probing atomic structure and Majorana wavefunctions in mono-atomic Fe-chains on super-conducting Pb-surface, npj. Quantum Inf 2016;2:16035.
[59] Nadj-Perge S, Drozdov K, Li J, Chen H, Jeon S, Seo J, et al. Observation of Majorana fermions in ferromagnetic atomic chains on a superconductor. Science 2014;346:602.
[60] Xu J-P, Wang M-X, Liu ZL, Ge J-F, Yang X, Liu C, et al. Experimental detection of a Majorana mode in the core of a magnetic vortex in-side a topological insulator-superconductor $Bi_2Te_3/NbSe_2$ heterostructure. Phys Rev Lett 2015;114:017001.
[61] Sengupta K, Žutić I, Kwon H-J, Yakovenko VM, Das Sarma S. Midgap edge states and pairing symmetry of quasi-one-dimensional organic superconductor. Phys Rev B 2001;63:144531.
[62] Fatin GL, Matos-Abiague A, Scharf B, Žutić I. Wireless Majorana bound states: from magnetic tunability to braiding. Phys Rev Lett 2016;117:077002.
[63] Matos-Abiague A, Shabani J, Kent AD, Fatin GL, Scharf B, Žutić I. Tunable magnetic textures: from Majorana bound states to braiding. Solid State Commun 2017;262:1.
[64] Braunecker B, Japaridze GI, Klinovaja J, Loss D. Spin-selective Peierls transition in interacting one-dimensional conductors with spin-orbit interaction. Phys Rev B 2010;82:045127.
[65] Tatara G, Fukuyama H. Resistivity due to a domain wall in ferromagnetic metal. Phys Rev Lett 1997;78:3773.
[66] Shabani J, Kjaergaard M, Suominen HJ, Kim Y, Nichele F, Pakrouski K, et al. Two-dimensional epitaxial superconductor-semiconductor heterostructures: a platform for topological superconducting networks. Phys Rev B 2016;93:155402.
[67] Kent AD, Worledge DC. A new spin on magnetic memories. Nat Nanotechnol 2015;10:187.
[68] Yang G, Stano P, Klinovaja J, Loss D. Majorana bound states in magnetic skyrmions. Phys Rev B 2016;93:224505.
[69] Güngördü U, Sandhoefner S, Kovalev AA. Stabilization and control of Majorana bound states with elongated skyrmions. Phys Rev B 2018;97:115136.
[70] Virtanen P, Bergeret FS, Strambini E, Giazotto F, Braggio A. Majorana bound states in hybrid two-dimensional Josephson junctions with ferromagnetic insulators. Phys Rev B 2018;98:020501(R).
[71] Kim SK, Tewari S, Tserkovnyak Y. Control and braiding of Majorana fermions bound to magnetic domain walls. Phys Rev B 2015;92:020412.
[72] Marra P, Cuoco M. Controlling Majorana states in topologically inhomogeneous superconductors. Phys Rev B 2017;95:140504.
[73] Kjaergaard M, Wölms K, Flensberg K. Majorana fermions in superconducting nanowires without spin-orbit coupling. Phys Rev B 2012;85:020503.
[74] Schüffelgen P, et al. Boosting transparency in topological junctions via stencil lithography, arXiv:1711.01665, preprint.
[75] Pientka F, Keselman A, Berg E, Yacoby A, Stern A, Halperin BI. Topological superconductivity in a planar Josephson junction. Phys Rev X 2017;7:021032.
[76] Hell M, Leijnse M, Flensberg K. Two-dimensional platform for networks of Majorana bound states. Phys Rev Lett 2017;118:107701.
[77] Ren H, Pientka F, Hart S, Pierce A, Kosowsky M, Lunczer L, et al. Topological superconductivity in a phase-controlled Josephson Junction, arXiv:1809.03076, preprint.
[78] Fornieri A, Whiticar AM, Setiawan F, Portoles Marin E, Drachmann ACC, Keselman A, et al. Evidence of topological superconductivity in planar Josephson junctions, arXiv:1809.03037, preprint.
[79] Boutin S, Lemyre JC, Garate I. Majorana bound state engineering via efficient real-space parameter optimization. Phys. Rev. B 2018;98:214512.
[80] Zhou T, Mohanta N, Han JE, Matos-Abiague A, Žutić I. Tunable magnetic textures in spin-valves: From spintronics to Majorana bound states, arXiv:1901.02506. Phys Rev B (in press).
[81] Ajayan P, Kim P, Banerjee K. Two-dimensional van der Waals materials. Phys Today 2016;69:38.
[82] Geim AK, Grigorieva IV. van der Waals heterostructures. Nature 2013;499:419.
[83] Cao Y, Fatemi V, Fang S, Watanabe K, Taniguchi T, Kaxiras E, et al. Unconventional superconductivity in magic-angle graphene superlattices. Nature 2018;556:43.
[84] Cao Y, Fatemi V, Demir A, Fang S, Tomarken SL, Luo JY, et al. Correlated insulator behaviour at half-filling in magic-angle graphene superlattices. Nature 2018;556:80.
[85] Gong C, et al. Discovery of intrinsic ferromagnetism in two-dimensional van der Waals crystals. Nature 2017;546:265.
[86] Huang B, et al. Layer-dependent ferromagnetism in a van der Waals crystal down to the monolayer limit. Nature 2017;546:270.
[87] Dent Y, et al. Gate-tunable room-temperature ferromagnetism in two-dimensional Fe_3GeTe_2. Nature 2018;563:94.
[88] O'Hara DJ, et al. Room temperature intrinsic ferromagnetism in epitaxial manganese selenide films in the monolayer limit. Nano Lett 2018;18:3125.
[89] Zhao C, et al. Enhanced valley splitting in monolayer WSe_2 due to magnetic exchange field. Nat Nanotechnol 2017;12:757.
[90] Zhong D, et al. Van der Waals engineering of ferromagnetic semiconductor heterostructures for spin and valleytronics. Sci Adv 2017;3:e1603113.
[91] Scharf B, Xu G, Matos-Abiague A, Žutić I. Magnetic proximity effects in transition-metal dichalcogenides: converting excitons. Phys Rev Lett 2017;119:129403.
[92] Lindemann M, Xu G, Pusch T, Michalzik R, Hofmann MR, Žutić I, Gerhardt NC, Ultrafast spin-lasers, arXiv:1807.02820. Nature (in press).
[93] Miller DAB. Attojoule optoelectronics for low-energy information processing and communications - a tutorial review. J Lightwave Technol 2017;3:346.

Igor Žutić is a Professor of Physics at the University at Buffalo. He received his Ph.D. in theoretical physics at the University of Minnesota in 1998, after undergraduate studies at the University of Zagreb, Croatia. His work spans topics from high-temperature superconductors, Majorana fermions, proximity effects, unconventional magnetism, and van der Waals materials, to prediction of various spin-based devices beyond the concept of magnetoresistance, including spin diodes, transistors, and lasers, which have been experimentally realized. With Jaroslav Fabian and Sankar Das Sarma he wrote a comprehensive article Spintronics: Fundamentals and Applications, for *Reviews of Modern Physics*, currently among the most cited articles on spin transport and magnetism. With Evgeny Tsymbal he is editing Spintronics Handbook: Spin Transport and Magnetism, Second Edition. Igor Žutić is a recipient of 2006 National Science Foundation CAREER Award, 2005 National Research Council/American Society for Engineering Education Postdoctoral Research Award. He is a Fellow of American Physical Society.